

**KU LEUVEN**



KU Leuven  
Department of Mechanical Engineering  
Celestijnenlaan 300B - box 2420  
B-3001 Heverlee (Belgium)

Proceedings of

**ISMA2012**

International Conference on  
**Noise and Vibration Engineering**

**USD2012**

International Conference on  
**Uncertainty in Structural Dynamics**



17 to 19 September, 2012  
Editors: P. Sas, D. Moens, S. Jonckheere

# Inverse identification and microscopic estimation of parameters for models of sound absorption in porous ceramics

**T. G. Zieliński**

Institute of Fundamental Technological Research, Polish Academy of Sciences

ul. Pawinskiego 5B, 02-106 Warszawa, Poland

e-mail: [tzielins@ippt.gov.pl](mailto:tzielins@ippt.gov.pl)

## Abstract

Samples of porous ceramics  $\text{Al}_2\text{O}_3$ , manufactured by a promising technology of gelcasting of cellular foams by using biopolymers as gel-formers, are examined in the impedance tube using the transfer function method. It is shown that the ceramics of total porosity around 90% forms an excellent sound absorbing material in the frequency range from 500 Hz to 6.4 kHz. Experimentally-determined curves of acoustic impedance and absorption are then used for inverse identification of relevant geometric parameters like: tortuosity, viscous and thermal permeability parameters and characteristic lengths. These parameters are required by some advanced models of sound propagation in rigid porous media, developed by Johnson, Koplik and Dashen, Champoux and Allard, with some variations introduced by Pride et al., and Lafarge et al. These models are utilized to produce curves of acoustic impedance and absorption that are used by the identification procedure which minimizes the objective function defined as a squared difference to the appropriate curves obtained experimentally. As a matter of fact, some experimental data are used for the determination of parameters while the other data – obtained for another sample of the same porous ceramics, yet having different thickness – serve for the validation purposes. Moreover, it is observed that the identified characteristic length for thermal effects corresponds very well to the average radius of pores, whereas the characteristic length for viscous forces is similar with the average size of “windows” linking the pores. The identification procedure minimises the objective function with respect to a set of some independent dimensionless parameters from which the actual model parameters can be calculated. In the definitions of the dimensionless parameters two reference frequencies are introduced – one relevant for viscous effects, the other for thermal effects. Such approach renders the optimization procedure very robust. In general, it is observed that, if the total porosity is known, simultaneous identification of the remaining model parameters is feasible by using only the objective function. In particular, the inverse identification allows to estimate the so-called static thermal permeability which in practice is not easy to determine by direct measurements, and thus, very often because of lack of this parameter, the simplified Lafarge model must be used which approximate this parameter with an analytical result obtained for a porous medium with circular cylindrical pores. Finally, a periodic microscopic cell consisting of a few pores representing an average morphology of porous ceramics is proposed and a finite-element analysis with periodic boundary conditions in order to estimate the static viscous permeability parameter is presented.

## 1 Introduction

There are several widely-used acoustic models of porous media, starting from the simple, purely phenomenological, model proposed by Delany and Bazely, and finishing with semi-phenomenological propositions by Johnson et al., which were later combined with the ones by Champoux and Allard, with some important variations proposed by Pride, Lafarge, and others [1]. All these models use some average macroscopic pa-

rameters, namely: the total porosity and flow resistivity (or permeability) – for the Delany-Bazely model – which are supplemented by the average tortuosity of pores and their characteristic dimensions – in the case of more advanced semi-phenomenological models. These models allow to describe the acoustic wave propagation in porous media in a wide frequency range, provided that the skeleton is rigid. However, using some formulas derived for these models with the Biot's theory of poroelasticity permits to describe correctly sound propagation in soft porous materials. Thus, the determination of the above-mentioned parameters is very important. For direct experimental measurements a specialistic equipment is required, different for various parameters. Therefore, an inverse identification based on the results of measurements of some global acoustical characteristics of a porous material is very tempting and should be tried in order to estimate the intrinsic parameters. Such attempts have been already performed: first, by using a simpler models, like Zwikker-Kosten description of porous material [2], and latter for the advanced Johnson-Champoux-Allard model [3, 4].

In the present work an inverse identification of the intrinsic parameters of the Johnson-Champoux-Allard model utilizes the curves of acoustic impedance measured in the impedance tube for samples of known thickness. This approach is similar with the one used in [4]. However, in the present paper a set of dimensionless parameters will be first defined with respect to the actual model parameters which should facilitate the identification procedure; and once the dimensionless parameters are identified, the model parameters can be easily calculated. Of some importance is the fact that two reference frequencies will be introduced in the definitions of the dimensionless parameters – one relevant for viscous effects, the other for thermal effects. Eventually, it will be also shown that some knowledge of micro-structural geometry of porous medium is very helpful to validate the estimation. Finally, a periodic microscopic cell consisting of a few pores representing an average morphology of porous ceramics will be proposed to serve for numerical analyses to estimate permeability parameters. The concurrence of such micro-scale derivation and inverse identification will be discussed.

## 2 Modelling sound absorption of porous materials

### 2.1 Models for sound propagation in porous media with rigid frame

When the skeleton of a porous medium can be assumed as rigid (which is common in materials like ceramic or metal foams and even in the case of softer foams in some frequency range), the time-harmonic acoustic wave propagation can be effectively modelled using the classical Helmholtz equation of linear acoustics:

$$\omega^2 \tilde{p} + c^2 \Delta \tilde{p} = 0, \quad (1)$$

where  $\omega = 2\pi f$  is the angular frequency of the propagating wave ( $f$  is the frequency),  $\tilde{p}$  is the (unknown) complex amplitude of acoustic pressure, and  $c$  is the speed of sound in the medium. This wave equation is valid for regions of space not containing any sources of acoustic energy. Thus, in case of such simplifying fluid-equivalent approach (that is, when a fluid layer is substituted for a layer of porous material) the material properties of porous medium must be somehow represented in equation (2) by one parameter only (the speed of sound  $c$ ). It is obvious, however, that in case of porous medium, this will be an effective quantity which should differ from the speed of sound of the fluid (typically, the air) filling the pores of porous material, even for materials of very high porosity (which is usually the case of sound proofing materials). Assuming that – as for inviscid isotropic elastic fluids:

$$c^2 = \frac{K}{\rho}, \quad (2)$$

where  $K$  and  $\rho$  are the bulk modulus and the density, respectively – it means that some effective bulk modulus and density must be specified for a virtual (homogenized) representation of porous material. Moreover, it is observed that porous materials are dispersive, therefore, the effective bulk modulus and density should be frequency-dependent functions:  $K = K(\omega)$  and  $\rho = \rho(\omega)$ .

The effective density of porous material must be somehow related to the density  $\rho_f$  of the actual fluid filling the pores; this is realized simply as follows:

$$\rho(\omega) = \rho_f \alpha(\omega), \quad (3)$$

where  $\alpha$  is a dimensionless function of frequency – the so-called dynamic (visco-inertial) tortuosity. It is greater than 1, which means that the effective density is bigger than the density of the fluid in pores, and thus, it accounts for the resistance forces between the fluid and the rigid skeleton of porous medium. It seems reasonable that the dynamic tortuosity, being a function of frequency, should depend on the visco-inertial properties of the pore-fluid and on some purely geometric characteristics of the skeleton. Johnson *et al.* [5] proposed a model, which – apart from the kinematic viscosity,  $\nu$ , of the fluid in pores – depends on four geometric parameters that macroscopically characterize a porous medium, namely: the total porosity,  $\phi$ , the (static) permeability,  $k_0$ , the tortuosity of pores,  $\alpha_\infty$ , and finally, the characteristic size of pores for viscous forces,  $\Lambda$ . The static permeability is an intrinsic property of the porous medium used, for example, in the Darcy's law, where it relates the pressure gradient and the flux, which – when divided by the total porosity – is equal to the (average, macroscopic) velocity of stationary-flow (therefore, at  $\omega = 0$ ). The tortuosity  $\alpha_\infty$  is defined as the ratio of the hypothetical effective density of a porous medium saturated by an ideal, inviscid fluid, to the density of this fluid. Therefore, it accounts only for inertial resistance, and in reality, when the saturating fluid is viscous, the effective density must only tend to the value  $\alpha_\infty \rho_f$  when the viscous skin depth tends to zero and the viscosity effects become negligible, that is when  $\omega \rightarrow \infty$ . The Johnson's model was modified by Pride *et al.* [6] and the improved version can be presented as follows:

$$\alpha(\omega) = \alpha_\infty + \frac{\nu}{i\omega} \frac{\phi}{k_0} \left[ \sqrt{\frac{i\omega}{\nu} \left( \frac{2\alpha_\infty k_0}{\Lambda \phi} \right)^2 + b^2 - b + 1} \right], \quad (4)$$

where  $b$  is a parameter introduced by Pride to adjust the low-frequency limit of the real part of the effective density (for circular pores this limit is obtained for  $b = 3/4$ ). Lafarge showed that the right low-frequency limit  $\alpha_0$  for the real part of  $\alpha$  (i.e.,  $\lim_{\omega \rightarrow 0} \text{Re } \alpha = \alpha_0$ ) is achieved when

$$b = \frac{2\alpha_\infty^2 k_0}{\Lambda^2 \phi (\alpha_0 - \alpha_\infty)}. \quad (5)$$

An analysis of thermal effects leads to the following expression for the effective bulk modulus

$$K(\omega) = \frac{P_0}{1 - \frac{\gamma - 1}{\gamma \alpha'(\omega)}}, \quad (6)$$

where  $P_0$  is the ambient mean pressure,  $\gamma$  is the heat capacity ratio for the pore-fluid (air), and  $\alpha'$  is the frequency-dependent thermal tortuosity. This function was introduced by Lafarge [7] as an analogue of the dynamic tortuosity. Similarly, the following model was proposed for this quantity:

$$\alpha'(\omega) = 1 + \frac{\nu'}{i\omega} \frac{\phi}{k'_0} \left[ \sqrt{\frac{i\omega}{\nu'} \left( \frac{2k'_0}{\Lambda' \phi} \right)^2 + b'^2 - b' + 1} \right]. \quad (7)$$

where  $\nu' = \nu/\text{Pr}$  with Pr being the Prandtl number of the pore-fluid, while  $k'_0$  is the static thermal permeability,  $\Lambda'$  is the characteristic size of pores for thermal effects, and finally  $b'$  is a parameter which can provide minor modifications of the effective bulk modulus in the low- and medium-frequency range; the low-frequency limit  $\alpha'_0$  for the real part of  $\alpha'$  (i.e.,  $\lim_{\omega \rightarrow 0} \text{Re } \alpha' = \alpha'_0$ ) is achieved when

$$b' = \frac{2k'_0}{\Lambda'^2 \phi (\alpha'_0 - 1)}. \quad (8)$$

Equations (3) and (6), together with the expressions (4) and (7), constitute a very effective model for sound propagation in porous media with rigid frame. This model involves eight parameters that in different ways depend on the micro-geometry of a porous material, yet are its average macroscopic properties; they are:  $\phi$ ,  $\alpha_\infty$ ,  $k_0$ ,  $k'_0$ ,  $\Lambda$ ,  $\Lambda'$ ,  $b$  (or  $\alpha_0$ ), and  $b'$  (or  $\alpha'_0$ ). However, by choosing that  $b = 1$ , or in consequence,  $\alpha_0 = \alpha_\infty + \frac{2\alpha_\infty^2 k_0}{\Lambda^2 \phi}$ , the simplified Johnson's model for dynamic tortuosity is achieved. A similar simplification can be done for the Lafarge model for thermal tortuosity by assuming that  $b' = 1$ , or  $\alpha'_0 = 1 + \frac{2k'_0}{\Lambda'^2 \phi}$ , thus, neglecting the possibility of some minor modifications in the low- and medium-frequency range. Eventually, the simplified version of the model, which involves only six geometrical parameters, can be written as follows:

$$\alpha(\omega) = \alpha_\infty + \frac{\nu}{i\omega} \frac{\phi}{k_0} \sqrt{\frac{i\omega}{\nu} \left( \frac{2\alpha_\infty k_0}{\Lambda \phi} \right)^2 + 1}, \quad \alpha'(\omega) = 1 + \frac{\nu'}{i\omega} \frac{\phi}{k'_0} \sqrt{\frac{i\omega}{\nu'} \left( \frac{2k'_0}{\Lambda' \phi} \right)^2 + 1}. \quad (9)$$

## 2.2 Surface impedance and acoustic absorption coefficient

Figure 1 shows the configuration of a layer of porous material of thickness  $\ell$  set to a rigid wall and under the excitation of a normally-incident, plane harmonic acoustic wave which propagates in the fluid (air) which also fills the pores of the porous layer. The wave penetrates into the layer and is fully reflected from the rigid wall. A standing-wave interference pattern results due to the superposition of forward- and backward-traveling waves. By measuring the sound pressure at two fixed locations it is possible to determine important acoustical characteristics of the material, namely, the complex-valued normal acoustic impedance and reflection coefficient, and the real-valued sound absorption coefficient. This is a typical configuration used in material testing.

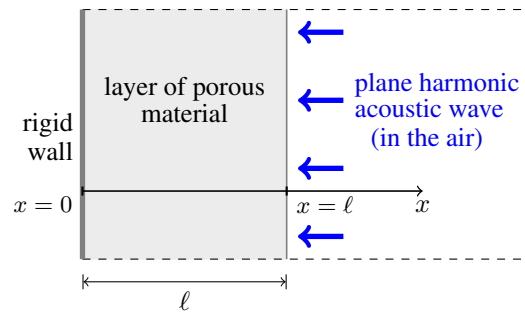


Figure 1: A layer of porous material set to a rigid wall – a typical configuration for acoustic material measurements

The problem depicted in figure 1 is one-dimensional and can be easily solved. Eventually, the formula for the surface impedance of a fluid or fluid-equivalent – for example, porous – layer of thickness  $\ell$  fixed to rigid wall can be derived [1]:

$$Z = \sqrt{\rho K} \frac{\exp(2i\omega\ell\sqrt{\rho/K}) + 1}{\exp(2i\omega\ell\sqrt{\rho/K}) - 1} = -i\sqrt{\rho K} \cot(\omega\ell\sqrt{\rho/K}) \quad (10)$$

Now, the reflection coefficient can be calculated [1]:

$$R(\omega) = \frac{Z(\omega) - Z_f}{Z(\omega) + Z_f}, \quad (11)$$

where  $Z_f$  is the characteristic impedance of fluid (air). Finally, knowing the reflection coefficient, the acoustic absorption coefficient can be determined:

$$A(\omega) = 1 - |R(\omega)|^2. \quad (12)$$

The quantities (10), (11), and (12) can be determined experimentally in the impedance tube in some frequency range (which depends on the size of the sample and tube), using the so-called two-microphone transfer function method.

### 3 Inverse identification of rigid skeleton parameters for acoustical modelling

#### 3.1 Dimensionless parameters

A methodology of parameter identification for the rigid-porous model, basing on some acoustical measurements carried out on rigid foams, will be now presented. For the purpose of the inverse identification procedure a set of independent, dimensionless parameters will be first defined. These parameters should be in an unequivocal relation with the model parameters and should render the optimization algorithm robust. Before such a set will be prescribed, one should notice that in all the expressions used by the models presented in the previous section the static viscous permeability,  $k_0$ , as well as the static thermal permeability,  $k'_0$ , appear always in fractional relation with the total porosity  $\phi$ , which by itself also appears only in this relation to one of those two permeability parameters. Thus, from the modelling perspective only two of those three parameters are independent. Therefore, one can expect that when using these models only the ratios  $k_0/\phi$  and  $k'_0/\phi$  may be identified unequivocally, which is not a serious drawback since they are actually used in modelling. Moreover, the total porosity is certainly the parameter which can be rather easily and correctly measured in direct way (especially, for porous materials with open-cell porosity, which is an issue here), and it is very often provided by the manufactures. Therefore, for the sake of simplicity, in what follows it will be assumed that the total porosity is known (and as a matter of fact, it was actually known for the samples used in the experimental tests). Thus, from the eight parameters which geometry of porous skeleton only seven need to be identified, namely:  $k_0$  (or  $k_0/\phi$ ),  $k'_0$  (or  $k'_0/\phi$ ),  $\alpha_\infty$ ,  $\Lambda$ ,  $\Lambda'$ ,  $\alpha_0$  (or  $b$ ), and  $\alpha'_0$  (or  $b'$ ); and eventually, there are only five parameters for the simplified version of the model (9), since the last two parameters are no longer used.

Let us define the following dimensionless parameters:

$$\begin{aligned} p_1 &= \alpha_\infty - 1, & p_2 &= \frac{\nu}{\omega_*} \frac{\phi}{k_0}, & p_3 &= \frac{\nu'}{\omega'_*} \frac{\phi}{k'_0}, \\ p_4 &= \frac{\omega_*}{\nu} \left( \frac{2\alpha_\infty k_0}{\Lambda \phi} \right)^2, & p_5 &= \frac{\omega'_*}{\nu'} \left( \frac{2k'_0}{\Lambda' \phi} \right)^2, \\ p_6 &= b = \frac{2\alpha_\infty^2 k_0}{\Lambda^2 \phi (\alpha_0 - \alpha_\infty)}, & p_7 &= b' = \frac{2k'_0}{\Lambda'^2 \phi (\alpha'_0 - 1)}. \end{aligned} \quad (13)$$

Here,  $\omega_* = 2\pi f_*$  and  $\omega'_* = 2\pi f'_*$ , where  $f_*$  and  $f'_*$  are some arbitrarily chosen reference frequencies for viscous and thermal dissipation effects, respectively; therefore, it seems obvious that  $f'_* < f_*$ , for example:  $f'_* = 1$  kHz and  $f_* = 3$  kHz; the choice of these frequencies will yet be discussed below.

Now, the formulas for dynamic viscous and thermal tortuosities,  $\alpha$  and  $\alpha'$ , can be rewritten in the following form:

$$\begin{aligned} \alpha(\omega) &= 1 + p_1 + \frac{\omega_*}{i\omega} p_2 \left[ \sqrt{\frac{i\omega}{\omega_*} p_4 + p_6^2 - p_6 + 1} \right], \\ \alpha'(\omega) &= 1 + \frac{\omega'_*}{i\omega} p_3 \left[ \sqrt{\frac{i\omega}{\omega'_*} p_5 + p_7^2 - p_7 + 1} \right]. \end{aligned} \quad (14)$$

After the dimensionless parameters are found, the model parameters can be calculated as follows:

$$\alpha_\infty = 1 + p_1, \quad k_0 = \frac{\nu}{\omega_*} \frac{\phi}{p_2}, \quad k'_0 = \frac{\nu'}{\omega'_*} \frac{\phi}{p_3},$$

$$\Lambda = \frac{2 + 2p_1}{p_2} \sqrt{\frac{\nu}{\omega_* p_4}}, \quad \Lambda' = \frac{2}{p_3} \sqrt{\frac{\nu'}{\omega'_* p_5}}, \quad \alpha_0 = 1 + p_1 + \frac{p_2 p_4}{2p_6}, \quad \alpha'_0 = 1 + \frac{p_3 p_5}{2p_7},$$
(15)

In case of the simplified version of model (9) only five dimensionless parameters need to be identified (since  $p_6 = b = 1$  and  $p_7 = b' = 1$ ) and then:

$$\alpha(\omega) = 1 + p_1 + \frac{\omega_*}{i\omega} p_2 \sqrt{\frac{i\omega}{\omega_*} p_4 + 1}, \quad \alpha'(\omega) = 1 + \frac{\omega'_*}{i\omega} p_3 \sqrt{\frac{i\omega}{\omega'_*} p_5 + 1}.$$
(16)

### 3.2 Objective function

The objective function for the parameter identification is defined as the sum – over the results obtained for the particular frequencies from the considered frequency range – of the squared differences between the acoustic impedance of porous sample measured in the impedance tube and this impedance calculated by using equation (10) and the parametric model discussed above, namely:

$$F(\mathbf{p}) = \sum_{\omega} |Z(\omega; \mathbf{p}) - Z_{\text{exp}}(\omega)|^2$$

$$= \sum_{\omega} \left[ (\text{Re } Z(\omega; \mathbf{p}) - \text{Re } Z_{\text{exp}}(\omega))^2 + (\text{Im } Z(\omega; \mathbf{p}) - \text{Im } Z_{\text{exp}}(\omega))^2 \right]$$
(17)

Here,  $\mathbf{p}$  is the vector of dimensionless parameters defined by (13) (depending on the model version – simplified or adjusted – there may be from 5 to 7 parameters),  $Z_{\text{exp}}(\omega)$  is the acoustic impedance measured at frequency  $\omega$  and  $Z(\omega; \mathbf{p})$  is its computed counterpart; as stated above, the summation ( $\sum_{\omega}$ ) is carried out over the discrete set of measuring/computational frequencies  $\omega$ , from the relevant frequency range. The acoustic impedance values are computed using equation (10) with the effective quantities  $\rho(\omega; \mathbf{p})$  and  $K(\omega; \mathbf{p})$  calculated using formulas (3) and (6) with relevant viscous and thermal tortuosities determined from equations (14), or equations (16) in case of the simplified model. One should notice that the analytical formulas for gradient of the objective function with respect to the parameters  $\mathbf{p}$  can be easily derived to be used by the minimization procedures.

This objective function will be minimized with respect to the dimensionless parameters  $\mathbf{p}$ . It is required that all the parameters are positive, however, some additional constraints may be imposed. For example, it is known that thermal dissipation effects are associated with the so-called thermal skin depth which tends to be bigger than the viscous skin depth corresponding to the viscous dissipation effects. Thus, the thermal effects are rather associated with the pore size while the viscous effects with the size of the “windows” linking the pores; therefore, in general, the viscous and thermal characteristic lengths should satisfy the following relation  $\Lambda \leq \Lambda'$ . Similarly, one may always expect that  $k_0 \leq k'_0$  which means that  $p_3 \leq \frac{\omega_*}{\omega'_*} p_2$ . Nevertheless, as will be demonstrated in the next section, the optimization algorithms with (simple) positive-value constraints and even the algorithms without constraints can be successfully used for correct identifications of model parameters.

### 3.3 Results of parameter identification for porous ceramics

Two samples of porous ceramics  $\text{Al}_2\text{O}_3$  – see figure 2(left) – with the known total porosity  $\phi = 90\%$ , had been prepared for experimental testing. The ceramics had been manufactured by a promising technology of



Figure 2: Two samples of ceramic foam  $\text{Al}_2\text{O}_3$  with porosity 90% (left), and the impedance-tube experimental set (right).

gelcasting of cellular foams by using biopolymers as gel-formers [8]. Both samples had been cut in the form of thick discs or cylinders with the diameter of 29 mm and they differed only by thickness: one of them was 18 mm thick and the other 24 mm. The samples were examined in the impedance tube – see figure 2(right) – using the transfer function method [9, 10]. Accordingly with the procedure, the ambient temperature and pressure were first measured to be used by the method for the speed of sound calculation in the air, and also to determine precisely some other properties, namely, the density and characteristic impedance of air – to be used later in the inverse identification algorithm and other calculations.

The acoustic impedance and reflection coefficient (both, real and imaginary parts), as well as the acoustic absorption coefficient were measured in the frequency range from 500 Hz to 6.4 kHz. Then, the experimentally-determined curves of acoustic impedance for the sample 18 mm thick were used for an inverse identification of the five model parameters of the (simplified) model of Johnson-Lafarge, namely: tortuosity  $\alpha_\infty$ , viscous and thermal permeabilities,  $k_0$  and  $k'_0$ , and two characteristic lengths – for viscous and thermal effects,  $\Lambda$  and  $\Lambda'$ , respectively. To this end, five dimensionless parameters,  $p_1, \dots, p_5$ , defined by formulas (3) were first identified by minimising the objective function (17). An optimization procedure with positive-value constraints applied for all five parameters was used, however, it was checked that the same results can be achieved using similar procedure without constraints. The initial (starting) value for all dimensionless parameters was 1.0, yet again it was verified that some other initial values (various for different parameters) gave usually the same final results which was one of the premises that it was not a local minimum that was attained. Only for some drastically different initial values a local minimum was attained, yet it was easily discerned using the validation reasoning described below. As a matter of fact, the dimensionless parameters were defined in such a way so that their realistic values were more or less of the same order, and moreover, so that the value 1.0 was a good starting point for the optimization procedure for all of them. To this end, the reference frequencies were introduced in their definitions as discussed in section 3.1. These frequencies play an important role in the scaling of the dimensionless parameters, however their choice may be within some limits rather arbitrary: it was verified that the same optimization results were obtained when  $f_* > f'_*$  and  $f_*$  was assigned some value from 2 kHz to 12 kHz, while  $f'_*$  from 0.5 kHz to 5 kHz; however, for some of the choices the optimization procedure lasted much longer. After the dimensionless parameters were identified, the model parameters were calculated using formulas (15). The identified values of dimensionless parameters are shown in figure 3 and the corresponding model parameters are listed in table 1, where the initial values for these parameters are also given (computed for the initial values  $p_1 = \dots = p_5 = 1$ , and  $f_* = 3$  kHz and  $f'_* = 1$  kHz).

The parameters identified as described above – that is, by using the optimization procedure which matched the impedance curves measured experimentally for the first sample ( $\ell = 18$  mm) with the ones calculated from the model – were then used to compute the impedance curves for the second sample ( $\ell = 24$  mm) and eventually compare them with the corresponding experimentally-determined curves. The acoustic absorption coefficient was also determined and used for the verification purposes. The surface acoustic impedance



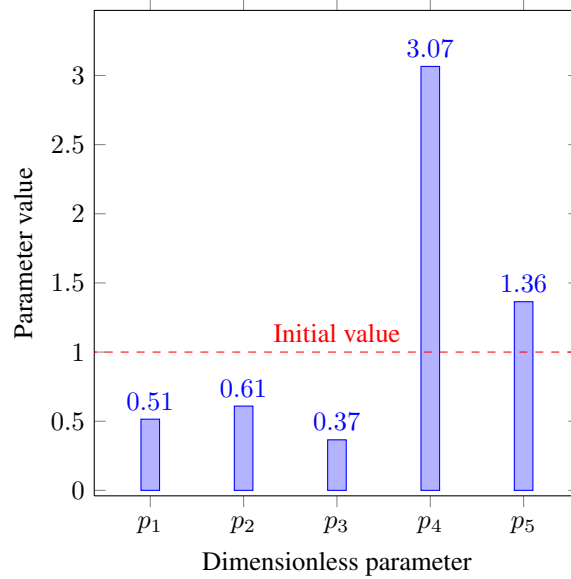


Figure 3: Identified values of dimensionless parameters

	$\alpha_\infty$	$k_0$ [m <sup>2</sup> ]	$k'_0$ [m <sup>2</sup> ]	$\Lambda$ [m]	$\Lambda'$ [m]
(a)	2.0000e+000	4.3456e-010	3.0603e-009	8.7895e-005	1.1662e-004
(b)	1.5149e+000	7.1304e-010	8.3739e-009	6.2392e-005	2.7323e-004
	Ratio (b) to (a)				
(c)	0.76	1.64	2.74	0.71	2.34

Table 1: The initial (a) and identified (b) values of model parameters, and the relevant ratios (c)

(real and imaginary parts) obtained for both samples are shown in figure 4, while the acoustic absorption coefficient is presented in figure 5. In fact, the impedance curves are presented in the form of a dimensionless ratio in reference to the constant characteristic impedance of air  $Z_f$  (i.e., the fluid occupying the pores and the impedance tube). It can be observed that the curves *modelled* for the sample 18 mm thick fit very well with their *measured* counterparts; it is rather obvious since the parameter identification was actually performed for this very sample. The consistency between the curves measured and modelled for the sample 24 mm thick is also good, however, some discrepancies are visible for the frequencies above 3 kHz, especially, for the imaginary part of the acoustic impedance. Nevertheless, the identification results are satisfactory and it is not by accident that the (acceptable) discrepancies are in the higher frequency range where the effect of a bigger pore situated on the sample surface is more vital. Moreover, another cause could be that the quality of the second sample was a bit inferior, especially with respect to the macro-homogeneity property which was well preserved by the first sample. There is, however, yet another coincidence which seems to validate the identification.

The ceramic foam samples were prepared using the technique described by Potoczek in [8] and their micro-geometric parameters (like average pore and “pore-window” sizes) should be very similar if not identical to the ones described in this paper for the foam of porosity  $89.9 \pm 0.3\%$  – see table 1 and figures 8(a) and 8(a) in [8]. Now, it is observed that the identified characteristic length for thermal effects corresponds very well to the average radius of pores, whereas the characteristic length for viscous forces is similar with the average radius of “windows” linking the pores, namely:  $2\Lambda = 125 \mu\text{m}$  and  $2\Lambda' = 546 \mu\text{m}$  from table 1 of the present paper agree very well with  $113 \mu\text{m}$  and  $529 \mu\text{m}$ , respectively, found in table 1 in [8]. This is a very important observation which validates the results of identification.

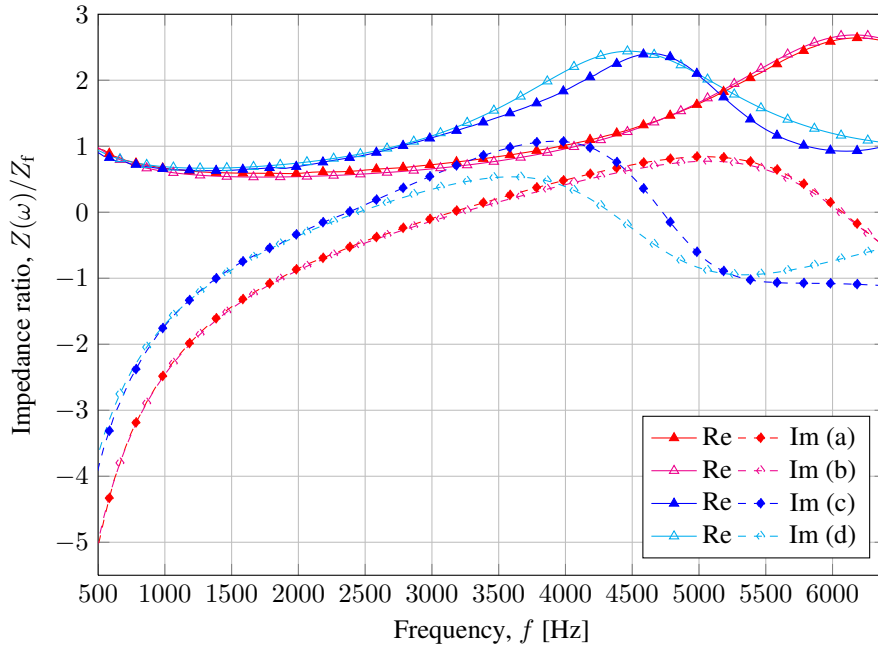


Figure 4: Curves of the impedance ratio  $Z(\omega)/Z_f$  – their real (Re) and imaginary (Im) parts – obtained for porous ceramic samples of thickness: 18 mm (a,b) and 24 mm (c,d). The curves (a,c) were found experimentally, whereas the curves (b,d) were computed from the model

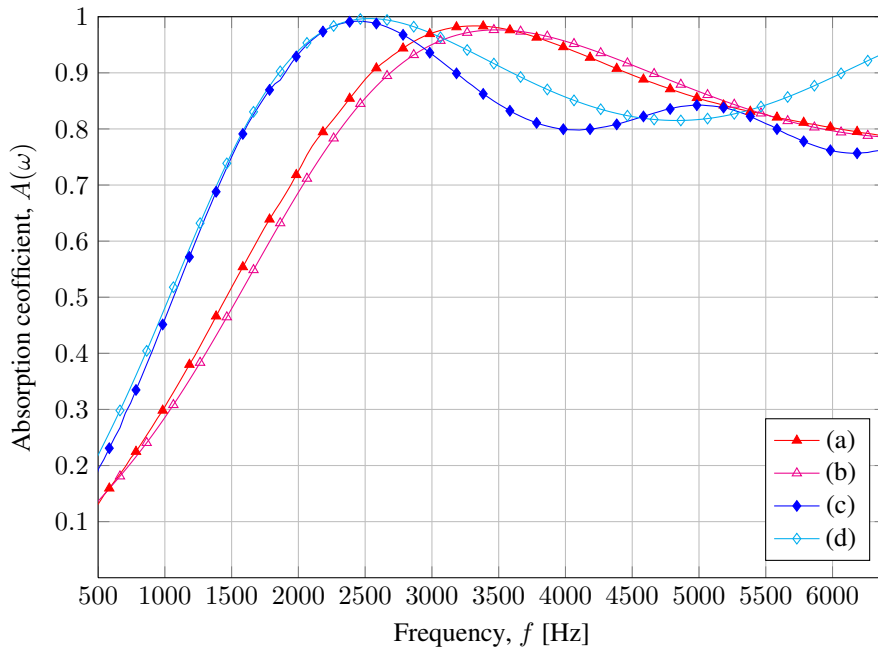


Figure 5: Acoustic absorption curves,  $A(\omega)$  – measured and modelled after parameter identification – for samples of porous ceramics of thickness: 18 mm (a,b) and 24 mm (c,d). The curves (a,c) were found experimentally, whereas the curves (b,d) were computed from the model

### 4 Microstructural analysis

Using the average radii of pores and/or windows found in [8] for ceramic foams of porosity 90%, periodic cells approximating micro-geometry of such foams can be constructed. An example of such a periodic cubic

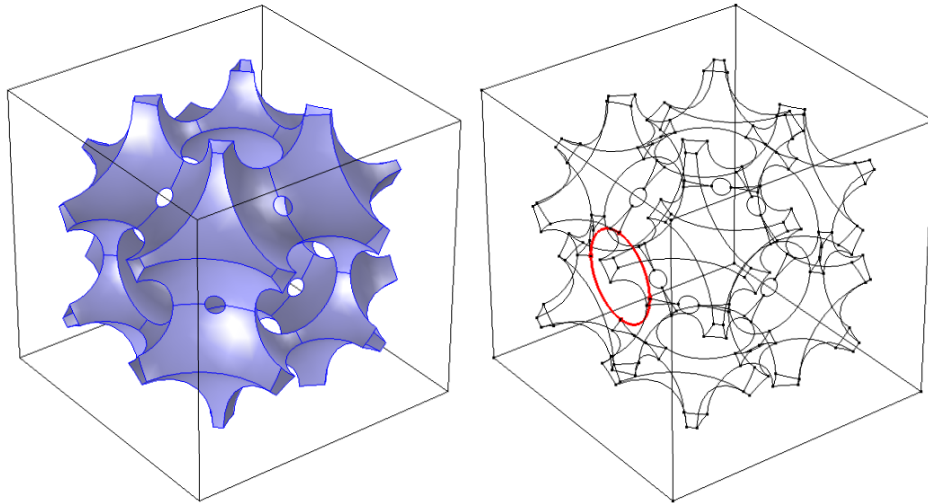


Figure 6: Periodic cell: the rigid skeleton boundaries (left) and a “wire-frame” view of its edges with the marked edge of one of the main windows linking the pores (right)

cell which contains eight pores of four different sizes is depicted in Figure 6, where the foam skeleton is visualized. The total volume of this periodic skeleton is 10% of the volume of the cube resulting in the designed porosity of 90%. The cell is not only periodic but also “isotropic” in the way that it is identical with respect to the three mutually-perpendicular directions. Therefore, from the macroscopic or macro-structural perspective it will exhibit purely isotropic behavior.

It is used for three-dimensional numerical analysis of the micro-macro transition approach for sound absorbing porous media [11, 12]. To this end, the multi-scale asymptotic method is applied [13], which permits to determine the macroscopic material description from knowledge of the physics and geometry at the microscopic level. In that way, for example, the so-called dynamic viscous permeability function  $k(\omega)$  can be computed by solving the periodic oscillating flow created in a porous medium by an external unit harmonic pressure gradient [11] and taking the average value from the velocity field over the computational fluid domain of the periodic cell; the flow is inviscid and incompressible and the velocity field in the pore is scaled in  $\text{m}^2$ . Such approach is relevant to sound propagation as long as the wavelength is large enough for the saturating fluid to behave as an incompressible fluid in volumes of the order of the homogenization volume [11, 12]. The permeability function is inversely proportional to the dynamic tortuosity function  $\alpha(\omega)$ , and in the limit  $\omega \rightarrow 0$ , it is equal to the static permeability  $k_0$ . Thus, to calculate the static permeability parameter, the corresponding steady Stokes problem need to be solved in the fluid domain of the periodic cell: this steady, inviscid, incompressible flow is driven by the unit vector of ‘pressure gradient’ [11].

The steady flow problem was solved for the periodic cell presented in figure 6. To this end, the finite element method was applied using the finite-element mesh of the fluid domain shown in figure 7. The flow permeability or rather ‘scaled velocity’ field was computed in the fluid domain with the no-slip boundary conditions applied on the skeleton boundaries and the periodic boundary conditions on the relevant pairs of the cell faces; as the final result – i.e., the static (macroscopic) permeability  $k_0$  – the fluid-phase average of the computed field was taken.

For the cubic cell as in figure 6, with the edge size of 0.4 mm, the window diameters are similar to some average values given in the work by Potoczek [8]. For example, the diameter of the window marked in figure 6(right) is 127  $\mu\text{m}$ . The static viscous permeability calculated in the way described above for such periodic cell was  $k_0 = 7.50 \times 10^{-10} \text{ m}^2$ , which is consistent with the value  $k_0 = 7.13 \times 10^{-10} \text{ m}^2$  (see table 1) found using the inverse identification procedure. However, it should be noticed that the considered periodic cell ensured exactly the total porosity of 90%, and approximately, the average size windows linking the pores. This size is very important for viscous effects considered here. The size of the pores, however, tend to be smaller than the average size given in [8]. It seems that some other features, like tortuosity, are

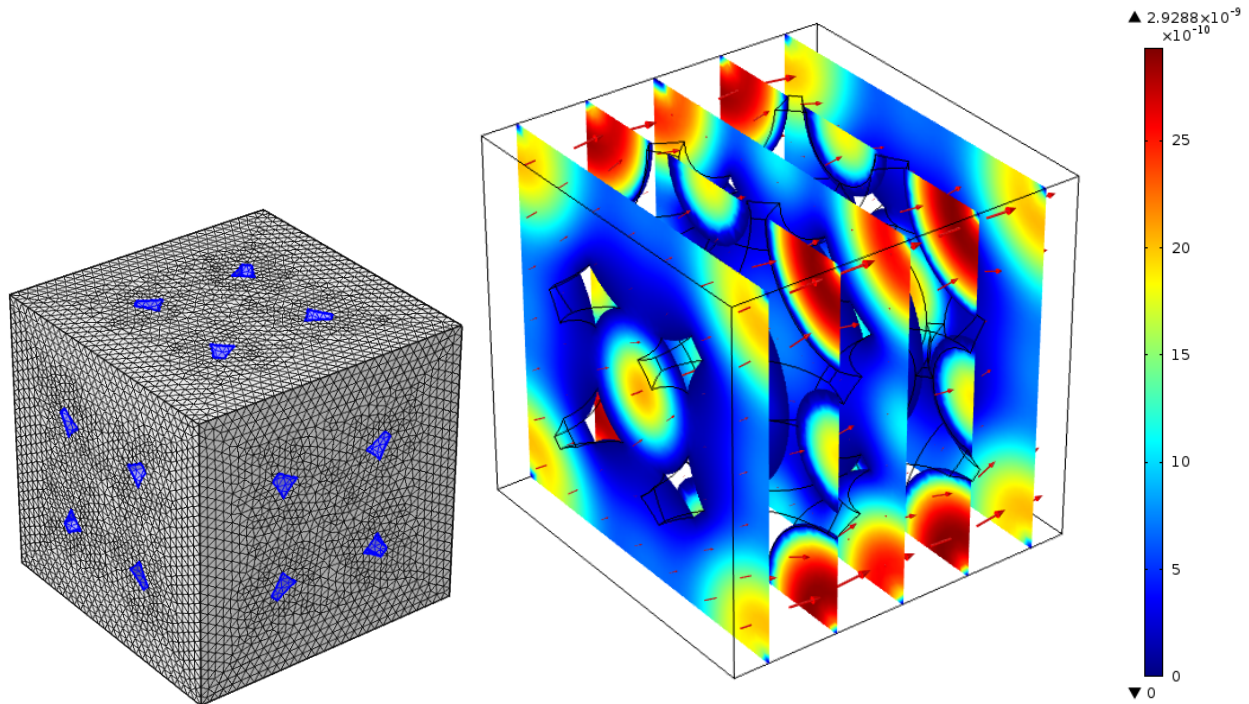


Figure 7: The finite-element mesh of the fluid domain (left) and the steady viscous incompressible flow through the periodic cell (right). The fluid-domain average of the shown ‘scaled velocity’ field [ $\text{m}^2$ ] is  $7.50 \times 10^{-10} \text{ m}^2$

not well reconstructed by this periodic skeleton. Thus, another cell should be constructed with a skeleton where the pore and window size should well represent the average values found by Potoczek [8] in actual ceramic foams. It seems not to be an easy task provided that – apart from the pore- and window-size requirement – the cell should be periodic and the total porosity should be exactly 90%. The tasks may be accomplished, however, yet perhaps by allowing for bigger cells – that is, the cells containing more pores; this should also permit to represent a more tortuous microstructure. On the other hand, bigger cells involve more computational effort to calculate permeability parameters, and moreover, one should remember to obey the size restriction for the representative volume element assumed during the homogenization procedure.

## 5 Conclusions

Two samples – of different thickness – made up of ceramic foam  $\text{Al}_2\text{O}_3$  of the known total porosity of 90% were tested in the impedance tube and the measured surface impedance curves were used by an inverse identification procedure to determine the remaining five parameters for the fluid-equivalent model of sound propagation in porous medium with rigid skeleton. To this end, a set of dimensionless parameters was first defined with respect to the actual model parameters. In the definitions two reference frequencies were introduced – one relevant for viscous effects, the other for thermal effects. Such approach rendered the optimization procedure (that was used to minimize the relevant objective function) very robust.

The identification was performed using the experimental results obtained for the first (thinner) sample. Assuming the known porosity all the remaining model parameters were identified. In particular, the inverse identification allowed to estimate the so-called static thermal permeability which in practice is not easy to determine by direct measurements, and thus, very often because of lack of this parameter, the simplified La-farge model must be used which approximate this parameter with an analytical result obtained for a porous medium with circular cylindrical pores.

The identification results were verified by comparing the impedance and absorption curves computed from the (identified) model for the second (thicker) sample, with the relevant curves found experimentally for this sample. The verification proved to be very satisfactory, though some small discrepancies were observed, however, in a higher frequency range, especially for the imaginary part of acoustic impedance, because of lesser quality of the second sample. In order to achieve more certain results several samples should be tested and the objective function for parameter identification should be taken as a sum of squared distance between the curves measured and computed from the model for all of the samples, or eventually, the final result can be taken as an average value from the values of a particular parameter identified for various samples.

Finally, it was observed that the identified characteristic length for thermal effects corresponds very well to the average radius of pores, whereas the characteristic length for viscous forces is similar with the average size of “windows” linking the pores. This was considered as a very important coincidence confirming the correctness of parameter identification. Certainly, the knowledge on micro-geometric parameters, like average or typical sizes of pores and windows linking the pores is of an uttermost importance since some of the model parameters are closely related to them (therefore can be used for verification). Moreover, on the basis on the micro-structural geometry – which is nowadays easily retrieved using, for example, computer tomography techniques – periodic cells (representative volume elements) can be constructed to be used by up-scaling homogenization/averaging methods which are able to calculate the parameters for macroscopic models directly from the micro-geometry of porous medium. Such an approach was carried out to estimate the static viscous permeability parameter.

## Acknowledgments

The author wishes to express his sincere gratitude to Dr. Marek Potoczek from Rzeszów University of Technology for providing samples of porous ceramics. Financial support of the Foundation for Polish Science Team Programme co-financed by the EU European Regional Development Fund Operational Programme “Innovative Economy 2007-626 2013”: Project “Smart Technologies for Safety Engineering SMART and SAFE”, No. TEAM/2008-1/4, and Project “Modern Material Technologies in Aerospace Industry”, No. 629 POIG.01.01.02-00-015/08, is gratefully acknowledged.

## References

- [1] J. F. Allard, N. Atalla, *Propagation of Sound in Porous Media: Modelling Sound Absorbing Materials*, Second Edition, Wiley (2009).
- [2] C. Braccési, A. Bracciali, *Least squares estimation of main properties of sound absorbing materials through acoustical measurements*, Appl. Acoust., Vol. 54, No. 1 (1998), pp. 59–70.
- [3] N. Sellen, M.-A. Galland, O. Hilbrunner, *Identification of the characteristic parameters of porous media using active control*, in: 8th AIAA/CEAS Aeroacoustics Conference, Breckenridge, CO, 17-19 June 2002, AIAA Paper 2002-2504 (2002).
- [4] Y. Atalla, R. Panneton, *Inverse acoustical characterization of open cell porous media using impedance tube measurements*, Canadian Acoustics, Vol. 33, No. 1 (2005), pp. 11–24.
- [5] D. L. Johnson, J. Koplik, R. Dashen, *Theory of dynamic permeability and tortuosity in fluid-saturated porous media*, J. Fluid Mech. 176 (1987) pp. 379–402.
- [6] S. R. Pride, F. D. Morgan, A. F. Gangi, *Drag forces of porous-medium acoustics*, Phys. Rev. B, Vol. 47, No. 9 (1993), pp. 4964–4978.

- 
- [7] D. Lafarge, P. Lemarinier, J. F. Allard, V. Tarnow, *Dynamic compressibility of air in porous structures at audible frequencies*, J. Acoust. Soc. Am., Vol. 102, No. 4, (1997), pp. 1995–2006.
- [8] M. Potoczek, *Gelcasting of alumina foams using agarose solutions*, Ceram. Int., Vol. 34 (2008), pp. 661–667.
- [9] *ISO 10534-2: Determination of sound absorption coefficient and impedance in impedance tubes* (1998).
- [10] J.-P. Dalmont, *Acoustic impedance measurement, Part I: A review. Part II: A new calibration method*, J. Sound Vib., Vol. 243, No. 3 (2001), pp. 427–459.
- [11] C. Perrot, F. Chevillotte, R. Panneton, *Bottom-up approach for microstructure optimization of sound absorbing materials*, J. Acoust. Soc. Am., Vol. 124, No. 2 (2008), pp. 940–948.
- [12] C. Perrot, F. Chevillotte, R. Panneton, *Dynamic viscous permeability of an open-cell aluminum foam: Computations versus experiments*, J. Appl. Phys., Vol. 103 (2008), pp. 024909–1–8.
- [13] C.-Y. Lee, M. J. Leamy, J. H. Nadler, *Acoustic absorption calculation in irreducible porous media: A unified computational approach*, J. Acoust. Soc. Am., Vol. 126, No. 4 (2009), pp. 1862–1870.